THE ASTROPHYSICAL JOURNAL, 206:85–99, 1976 May 15

ABUNDANCES OF SIMPLE OXYGEN-BEARING MOLECULES AND IONS IN INTERSTELLAR CLOUDS

A. E. GLASSGOLD
New York University
AND
WILLIAM D. LANGER
New York University and Goddard Institute for Space Studies
Received 1974 July 29; revised 1975 October 9

ABSTRACT

The abundances of simple oxygen-bearing interstellar molecules in warm ($T \gtrsim 40$ K), diffuse, and moderately thick clouds are calculated on the basis of binary gas phase reactions. The most important reactions are ion-molecule, charge exchange, and dissociative recombination reactions, as suggested mainly by earlier workers. The progenitor of these molecules in diffuse clouds is the cosmic ray produced H^+ ion, working through the charge exchange reaction with O. The ionization of H^+ and He^+ are also discussed. Dissociative charge exchange of He^+ with H_2 is an important source of H^+ in regions of large fractional abundance of H_2, as well as an important destruction mechanism for He^+ even for small f ($\gtrsim 0.1$). The calculated molecular abundances are consistent with some of the available observational information.

Subject headings: atomic processes — interstellar: molecules — nebulae: abundances

I. INTRODUCTION

The theory of molecule formation remains as a basic problem in the interstellar medium. Two main mechanisms have been considered, formation on grains and binary gas phase reactions. Grain formation is generally believed to be responsible for the formation of H_2, but its role for other molecules is unclear. (See Watson and Salpeter 1972*a*, *b* for the most recent and complete account of this subject and for other references to the literature.) The prospects for gas phase reactions have been greatly enhanced by the recent focus on ion-molecule reactions (Solomon and Klemperer 1972; Herbst and Klemperer 1973; Watson 1973*a*, *b*, 1974; Dalgarno, Oppenheimer, and Berry 1973; Black and Dalgarno 1973*a*, *b*).

In this paper we calculate the abundances of simpler oxygen-bearing molecules on the basis of various ion-molecule and dissociative recombination reactions. Most of these reactions have already been mentioned by Watson and by Dalgarno and his collaborators. We integrate and extend the work of the above-mentioned authors by simultaneously treating the most important production and destruction processes required for calculating the abundances of CO, OH, and H_2O. This treatment necessitates inclusion of HCO and the ions O^+, OH^+, H_2O^+, H_3O^+, CO^+, and HCO^+. The abundances of electrons and other positive ions also play an important role in quantitative abundance estimates. The H^+ and He^+ abundances are coupled by the dissociative charge exchange of He^+ with H_2. This reaction is an important source of H^+ in regions with large fractional abundances of molecular hydrogen, $f = 2n(H_2)/n$ [$n = n(H) + 2n(H_2)$], and is a major loss mechanism for He^+ even for small ($\gtrsim 0.1$). A detailed discussion of the abundances of these ions and electrons is given in Appendix A. The considerations of this paper are restricted to diffuse and moderately thick clouds with column densities $\lesssim (3\text{–}4) \times 10^{21}$ cm^{-2}, and to warm regions ($T \gtrsim$ 30–40 K) with densities $n \lesssim 10^3$ cm^{-3}. The latter restrictions are such that radiative association reactions can be neglected for producing oxygen-bearing molecules. The hydrogen in the center of these clouds is predominantly molecular, and other molecules are also present but at much lower abundances than in thicker and denser clouds. The calculations will be discussed in § II, and some comparisons with the small amount of relevant experimental information will be given in § III.

II. CALCULATION

The reactions which form the basis of our calculation are grouped together in Tables 1, 2, and A1. The reactions which are needed to establish the abundances relative to O of O^+, OH^+, OH, H_2O^+, H_2O, and H_3O^+ are listed in Table 1. Those required for calculating the abundances of CO^+, CO, HCO^+, and HCO are given in Table 2. Table A1 in the Appendix presents the reactions which occur in the ionization balance.

Many gas phase as well as grain-catalyzed reactions have been omitted in the tables. We made our selection on the basis of whether or not a particular reaction makes a significant contribution to the production and destruction rates for the molecules and regions of concern in this work. Thus a reaction may be ignored

because a rate constant and/or reactant density is small. For example, we ignore reactions with H_3^+, such as $H_3^+ + H_2O \rightarrow H_3O^+ + H_2$, which has a measured rate constant $K \approx 3 \times 10^{-9}$ cm^3 s^{-1} (Burt *et al.* 1970). The ratio of the rate at which this reaction destroys H_2O to that for photodestruction of H_2O with rate $G(H_2O)$ can be estimated as

$$Kn(H_3^+)/G(H_2O) \lesssim 10^6 \zeta_2(H_2^+) T^{1/2} \exp[\tau_{gr}(H_2O)]/x_e ,$$

where $\tau_{gr}(H_2O)$ is the optical depth for grain absorption in the wavelength range important for photodissociation of H_2O, and $\zeta_2(H_2^+)$ is the cosmic-ray production rate of H_2^+ from H_2. This ratio is negligible for the clouds considered here because it does not approach unity until very large values for the optical depth $\tau_{gr}(H_2O)$ are reached. [Note that $\tau_{gr}(H_2O) \approx N(1.33 \times 10^{21}\ \text{cm}^{-2})^{-1}$.] In thicker and denser interstellar clouds, H_3^+ plays a major role in molecule formation (Herbst and Klemperer 1973). The ratio of the rate of molecule production initiated by H^+ to that initiated by H_3^+, $k_5 x(H^+)/Kx(H_3^+)$, can be estimated for $f \rightarrow 1$ using equations (A4) and (A5) in Appendix A. The result is $10^2 e^{-232/T}/(10^{-2} + e^{-232/T})$, and thus H^+ production dominates for $T \gtrsim 30$ K. This estimate has been based on the assumption, appropriate to diffuse clouds, that the electron density

TABLE 1

OXYGEN MOLECULE FAMILY REACTIONS

Reaction	Rate*	Reference†
Charge Exchange		
$H^+ + O \rightarrow O^+ + H$	$k_5 = 10^{-9} e^{-232/T}$	1
$O^+ + H \rightarrow H^+ + O$	$k_6 = 10^{-9}$	1
$H^+ + OH \rightarrow OH^+ + H$	$k_{10} = 10^{-9}$	HK
$He^+ + OH \rightarrow OH^+ + He$	$k_{11} \approx 2 \times 10^{-10}$	...
$H^+ + H_2O \rightarrow H_2O^+ + H$	$k_{13} = 10^{-9}$	HK
$He^+ + H_2O \rightarrow H_2O^+ + He$	$k_{14} \approx 1.7 \times 10^{-10}$	3
Ion-Molecule		
$O^+ + H_2 \rightarrow OH^+ + H_2$	$k_8 = 1.6 \times 10^{-9}$	2
$OH^+ + H_2 \rightarrow H_2O^+ + H$	$k_{15} = 1.0 \times 10^{-9}$	2
$H_2O^+ + H_2 \rightarrow H_3O^+ + H$	$k_{16} = 0.6 \times 10^{-9}$	2
$C^+ + OH \rightarrow CO^+ + H$	$k_{17} \approx 10^{-9}$	...
$C^+ + OH \rightarrow CO + H^+$	$k_{18} = 2 \times 10^{-9}$	HK
$C^+ + H_2O \rightarrow HCO^+ + H$	$k_{19} = 2 \times 10^{-9}$	3
$C^+ + H_2O \rightarrow HCO + H^+$	$k_{20} < 3 \times 10^{-11}$	5
$He^+ + OH \rightarrow$ all products‡	$k_{21} \approx 4 \times 10^{-10}$	...
$He^+ + H_2O \rightarrow$ all products‡	$k_{22} = 4.5 \times 10^{-10}$	3
Dissociative Recombination*		
$e + OH^+ \rightarrow O + H$	$\beta_2(OH^+) \approx 5 \times 10^{-7}$	...
$e + H_2O^+ \rightarrow$ all products§	$\beta_3(H_2O^+) \approx 10^{-6}$	...
$e + H_3O^+ \rightarrow$ all products	$\beta_4(H_3O^+) = 2 \times 10^{-6}$	4
Photodestruction		
$h\nu + OH \rightarrow O + H$	$G_d(OH) = 2.5 \times 10^{-10}$ s^{-1}	...
$h\nu + OH \rightarrow OH^+ + e$	$G_i(OH) \ll G_d(OH)$	...
$h\nu + H_2O \rightarrow$ all channels	$G(H_2O) \approx 5 \times 10^{-10}$ s^{-1}	...
$h\nu + H_2O \rightarrow OH + H$	$G_d(H_2O \rightarrow OH) \approx 4 \times 10^{-10}$ s^{-1}	...
$h\nu + H_2O \rightarrow H_2O^+ + e$	$G_i(H_2O) \approx 3 \times 10^{-11}$ s^{-1}	...

* All reaction rates are in units of cm^3 s^{-1} unless otherwise noted.

† Numerical values of rate constants without references have been estimated or guessed by the present authors. When ion-molecule rate constants have been previously estimated by Herbst and Klemperer 1973, we use their values and label them by the notation HK.

‡ Some of the channels for $He^+ + OH$ and $He^+ + H_2O$ are dissociative charge exchanges which we have not listed separately, since their branching ratios are not known or required.

§ The notation $\beta_3(H_2O^+)$ indicates, for example, the total recombination rate to all channels. When the branch $e + H_2O^+ \rightarrow OH + H$ is required, we denote its rate constant as $\beta_3(H_2O^+ \rightarrow OH)$. A similar notation applies to photo-processes.

REFERENCES.—
1. Field and Steigman 1971.
2. Kim, Theard, and Huntress 1975.
3. Bolden and Twiddy 1972.
4. Leu *et al.* 1973*a*.
5. Huntress 1976.

$x_e \approx 10^{-4}$. In thicker clouds, where x_e is much less, H_3^+ production is more important.

The essential point of view in this work is that the formation of the most abundant heavy molecules in warm, moderately diffuse clouds, i.e., CO, OH, and H_2O, can be treated by considering only the two restricted classes of reactions given in Tables 1 and 2. The former refers to the simplest O,H family of molecules, which contain a single oxygen atom and varying numbers of H atoms and ions. The latter refers to the simplest C, O, and C,O,H families which contain molecules with a single O and a single C atom, and not more than one H atom or ion. The two groups of molecules are rather simply connected for diffuse clouds. When we examine Table 2, we see that the CO^+, CO, HCO^+, and HCO densities can be expressed in terms of the densities of OH and H_2O, and that there are no other direct links with the O,H family.

Reactions with the CH family will also contribute to the abundances of molecules containing C, O, and H, but not OH or H_2O. The formation of CH and CH_2 can be initiated by radiative association of C^+ with H (see Solomon and Klemperer 1973) or with H_2 (Black and Dalgarno 1973*b*). The production of CO, HCO^+, etc., proceeds by neutral molecule reactions with oxygen at a rate $\sim 3 \times 10^{-11}$ cm^3 s^{-1}. Langer (1976*a*) has considered the relative importance of the various ion-molecule reactions for CO production in thicker clouds. For diffuse clouds, we find that the ratio of molecule production by H^+ charge exchange to that by C^+ radiative association is $\sim(10^4/n)e^{-232/T}/(10^{-2} + e^{-232/T})$, using $\zeta_p \approx 10^{-17}$ s^{-1} and the radiative association rate constant $\sim 10^{-16}$ cm^3 s^{-1}. For temperatures $T \gtrsim 40$ K and $n \lesssim 10^3$ cm^{-3} we can neglect radiative association as a production mechanism of oxygen-bearing molecules.

Some remarks are in order regarding the values of the rate constants listed in Tables 1 and 2. Measurements of the reactions have been made in only about 40 percent of the cases. By using theoretical calculations and by applying conventional wisdom for each class of reaction, we can reduce the serious gaps in our knowledge of rate constants to just a few reactions. In

TABLE 2

CARBON MONOXIDE FAMILY REACTIONS

Reaction	Rate*	Reference†
Ion-Molecule		
$C^+ + OH \rightarrow CO^+ + H$	$k_{17} = 1.0 \times 10^{-9}$	...
$C^+ + OH \rightarrow CO + H^+$	$k_{18} = 1.0 \times 10^{-9}$	HK
$C^+ + H_2O \rightarrow HCO^+ + H$	$k_{19} = 2 \times 10^{-9}$	3
$C^+ + H_2O \rightarrow HCO + H^+$	$k_{20} < 3 \times 10^{-11}$	5
$CO^+ + H_2 \rightarrow HCO^+ + H$	$k_{24} = 1.4 \times 10^{-9}$	2
Charge-Exchange		
$CO^+ + H \rightarrow CO + H^+$	$k_{23} \approx 10^{-9}$	...
Dissociative Charge Exchange		
$He^+ + CO \rightarrow C^+ + O + He$	$k_{25} = 1.6 \times 10^{-9}$	6
Dissociative Recombination		
$e + CO^+ \rightarrow O + C$	$\beta_5 \approx 5 \times 10^{-7}$	...
$e + HCO^+ \rightarrow$ all channels‡	$\beta_6(HCO^+) = 5 \times 10^{-7}$ (for 80 K)	7
Photodestruction		
$h\nu + CO \rightarrow C + O$	$G(CO) = 3.0 \times 10^{-12}$ s^{-1}–2×10^{-11} s^{-1}	8
$h\nu + HCO \rightarrow$ all channels	$G(HCO) = 8 \times 10^{-9}$ s^{-1}	...
$h\nu + HCO \rightarrow HCO^+ + e$	$G_i(HCO) \ll G(HCO)$	...

* All reaction rates are in units of cm^3 s^{-1} unless otherwise noted.

† Numerical values of rate constants without references have been estimated or guessed by the present authors. When ion-molecule reaction rates have been previously estimated by Herbst and Klemperer 1973, we use their values and label them by the notation HK.

‡ The notation $\beta_6(HCO^+)$ indicates, for example, the total recombination rate to all channels. When the branch $e + HCO^+ \rightarrow CO + H$ is required, we denote its rate constant as $\beta_6(HCO^+ \rightarrow CO)$. A similar notation applies to photo-processes.

REFERENCES.—
1–5. See Table 1.
6. Laudenschlager, Huntress, and Bowers 1974.
7. Leu *et al.* 1973*b*.
8. Solomon and Klemperer 1972 (see text).

this work the most important is the photodissociation rate of CO. In the following we present a brief discussion of the various types of reactions and the basis for our choices of rate constants. In the tables the letters HK indicate that no experimental value or theoretical calculation exists and that we have adopted the value given by Herbst and Klemperer (1973). No reference means that neither source is available and that the value listed is our own guess.

a) Ion-Molecule Reactions

Extensive measurements (reviewed by Ferguson 1973) support the general rule that exothermic ion-molecule reactions have rate constants $\sim 10^{-9}$ cm^3 s^{-1}. This rule probably works best for the total rate constant, i.e., the branching ratios are less certain. However, where we did have to assume branching ratios ($k_{17}/k_{18} = 1/2$), they were not important for the main conclusions of this paper on the abundances of CO, OH, and H_2O. For example, both branches $C^+ + H_2O \rightarrow HCO^+ + H$ and $C^+ + H_2O \rightarrow HCO + H^+$ lead to CO when the further reactions of HCO^+ and HCO are taken into account. On the other hand, the HCO^+ : HCO ratio is affected by this branching ratio.

b) Charge Exchange

Exothermic charge exchange reactions involving molecules or molecular ions also tend to have large reaction constants $\sim 10^{-9}$ cm^3 s^{-1} at thermal energies. We have adopted this value for the three charge exchange reactions $H^+ + OH$, $H^+ + H_2O$, and $CO^+ + H$. Again, an analysis of the fate of the reaction products shows that these reactions are not crucial for our main qualitative conclusions. For example, the OH^+ and H_2O^+ ions which result from the first two reactions are largely converted back to OH and H_2O by subsequent ion-molecule reactions with H_2 and dissociative recombinations with electrons. The charge exchange reaction $H^+ + O \rightarrow O^+ + H$ is endothermic by $\Delta E = 232$ K. Experiments for $T \gtrsim 300$ K give a large rate constant (Fehsenfeld and Ferguson 1972), but no measurements are available at the low temperatures of interest in molecular hydrogen clouds ($T \lesssim 100$ K). The values given in Tables 1 and A1 for this reaction are those calculated by Field and Steigman (1971). The theory of charge exchange becomes very difficult when $kT \approx \Delta E$ (see the critical comments by Weisheit 1973), so that additional theoretical and experimental work on this reaction would be very useful.

c) Dissociative Recombination

The total recombination rates for H_3O^+ and HCO^+ have been measured by Leu *et al.* (1973*a*, *b*). We have assumed that

$$\beta_2(OH^+)/\beta_3(H_2O^+) = \beta_3(H_2O^+)/\beta_4(H_3O^+) = \tfrac{1}{2},$$

but this assumed decrease in rate constant with complexity of the ion is not critical, since both OH^+ and H_2O^+ are destroyed more rapidly by ion-molecule reactions with H_2 than by dissociative recombination. A more critical question is the branching ratio such as $\beta_4(H_3O^+ \rightarrow OH)/\beta_4(H_3O^+ \rightarrow H_2O)$, which bears directly on the abundance ratio of H_2O/OH. We will give some illustrations of the effect of changing these branching ratios when we present our results in § III.

d) Photodestruction

Water ($I = 12.6$ eV, $D = 5.1$ eV).—Among the molecules of interest here, the experimental situation appears to be the best for H_2O according to Hudson's (1972) critical review of ultraviolet photoabsorption cross sections. We calculated the values in Table 1 for the total photodestruction rate $G(H_2O)$ and the photoionization rate $G_i(H_2O)$ by integrating the cross sections given by Hudson with the "Jura-Habing" radiation field given in Figure 1 of Glassgold and Langer (1974). Stief *et al.* (1972) gave a similar value for $G_d(H_2O)$. It may be noted that $G_i/G \approx 0.06$. There is no reason to believe that any branch other than $H_2O \rightarrow OH + H$ contributes importantly to photodissociation when $\lambda > 912$ Å.

The hydroxyl radical ($I = 13.2$ eV, $D = 4.35$ eV).—Smith and Stella (1975) estimate from their studies of radiative lifetimes of OH that $G_d(OH) \gtrsim 10^{-10}$ s^{-1} for the Jura (1974*b*) radiation field. The actual rate is likely to be larger, and we have adopted the rate $G_d(OH) = 2.5 \times 10^{-10}$ s^{-1}. Because of the proximity of the ionization potential to the Lyman edge, it is very likely that $G_i(OH) \ll G_d(OH)$, and we ignore photoionization.

Carbon monoxide ($I = 14.0$ eV, $D = 11.1$ eV).—Experimental information is available for CO but not without uncertainties, as discussed by Hudson (1971) and by Solomon and Klemperer (1972). Solomon and Klemperer based their estimates on a continuum photodissociation cross section of $\sim 10^{-17}$ cm^2 for the range 912 Å $< \lambda <$ 960 Å (the threshold for CO dissociation is 1120 Å) and an effective dissociating transition at 1050 Å with $f = 4 \times 10^{-3}$. Adjusted for the radiation field of Jura (1974*b*), we estimate $G(1050\text{ Å}) = 3 \times 10^{-12}$ s^{-1} and $G(\lambda < 960\text{ Å}) \approx 1.5 \times 10^{-11}$ s^{-1}. Hudson (1971) has emphasized that the reported absorption continuum beginning at 960 Å is probably due to band overlap, and so we regard the estimate of this contribution as an upper limit. In accord with the uncertainty in G(CO) arising from our lack of knowledge concerning the transitions and the nature of the ultraviolet radiation field beyond the Lyman edge, we will discuss the effects of varying G(CO) on the results presented below in § III.

The formyl radical ($I = 9.9$ eV, $D = 1.2$ eV).—The small dissociation energy suggests that photodissociation will be the main destruction mechanism for HCO. We have made a rough estimate for purposes of orientation by assuming a constant cross section of 10^{-17} cm^2 and a mean spectral energy density of 5×10^{-17} ergs cm^{-3} Å^{-1}, and find $G(HCO) \approx 8 \times 10^{-9}$ s^{-1}. We also expect that $G_i(HCO) \ll G(HCO)$ on the basis of the relatively large ionization potential.

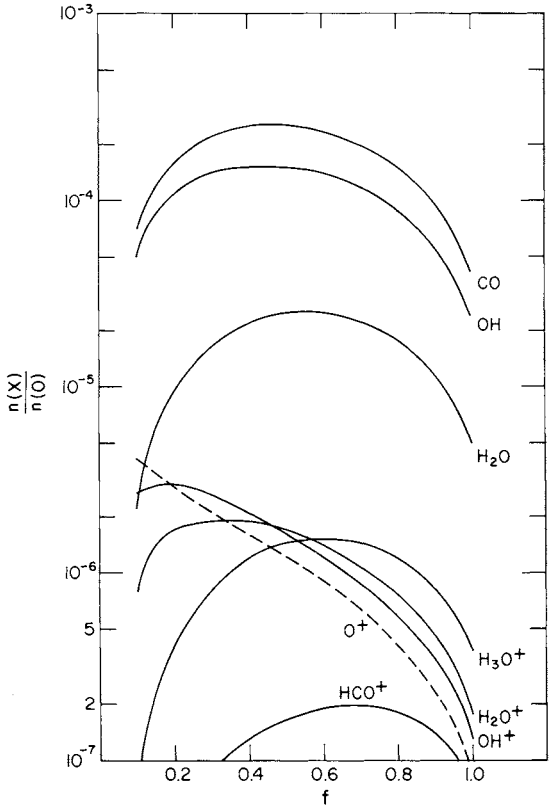

FIG. 1.—Density ratios of species X (labeled on curves) to atomic oxygen (O) as a function of molecular hydrogen ratio $f = 2n(H_2)/n$. The reaction rate constants and other parameters are given in Tables 1–3, and Table A1 (e.g., $T = 80$ K, $n = 100\ \mathrm{cm}^{-3}$).

The steady-state balance equations may be obtained from the reactions listed in Tables 1 and 2 by equating the production and destruction rates for each species. The results are listed in Appendix B, where we use the notation $f = 2n(H_2)/n$, $x_i = n_i/n$, and $n = n(H) + 2n(H_2)$.

The solution of this system of equations together with the ionization balance equations of Appendix A are illustrated in Figure 1. The abundances relative to O are plotted as a function of $f = 2n(H_2)/n$ for fixed density $n = 100\ \mathrm{cm}^{-3}$ and fixed temperature $T = 80$ K, the latter representing the mean temperature of the diffuse clouds observed by OAO-3 (Spitzer and Cochran 1973; Spitzer, Cochran, and Hirshfeld 1974). These parameters, together with rate constants that have not yet been specified, are summarized in Table 3. The complete set of parameters and rate constants given in Tables 1–3 and A1 define what we shall later refer to as our "standard run." The choice of cosmic-ray ionization rate is discussed in Appendix A and the effects of varying ζ_p will be taken up below. The humpbacked shape of the molecular abundance curves in Figure 1 occurs for the following reasons: (1) the abundances are rapidly increasing functions of f for small f because the molecules are formed by ion-molecule reactions with H_2; (2) they decrease for large

TABLE 3

CLOUD PARAMETERS AND RATE CONSTANTS FOR THE STANDARD RUN

Physical parameters:
$n = 100\ \mathrm{cm}^{-3}$
$T = 80$ K
$\zeta_p = 1 \times 10^{-17}\ \mathrm{s}^{-1}$
Rates for photodestruction:
$G(\mathrm{CO}) = 10^{-11}\ \mathrm{s}^{-1}$
$G_d(\mathrm{OH}) = 2.5 \times 10^{-10}\ \mathrm{s}^{-1}$
$G_i(\mathrm{OH}) = 0$
$G_i(\mathrm{HCO}) = 0$
Optical depths for grain attenuation:
$\tau_{gr}(\mathrm{CO}) = N/(8 \times 10^{20}\ \mathrm{cm}^{-2})$
$\tau_{gr}(\mathrm{H_2O}) = N/(1.33 \times 10^{21}\ \mathrm{cm}^{-2})$
$\tau_{gr}(\mathrm{OH}) = N/(1 \times 10^{21}\ \mathrm{cm}^{-2})$
Branching ratios:
$\beta_4(\mathrm{H_3O^+} \rightarrow \mathrm{OH}) = \beta_4(\mathrm{H_3O^+} \rightarrow \mathrm{H_2O})$
$\beta_3(\mathrm{H_2O^+} \rightarrow \mathrm{OH}) = \beta_3(\mathrm{H_2O^+})$
Abundances:
$\xi_C = 7 \times 10^{-5}$
$\xi_O = 2 \times 10^{-4}$
$\zeta_{He} = 1/12$

f because $x(H^+)$ decreases as $f \rightarrow 1$, as discussed in Appendix A. This decrease is reflected in the O^+ abundance in Figure 1. Molecule formation for $f > 0.9$ would be as much as 5 times smaller had we failed to include H^+ production from the reaction $He^+ + H_2 \rightarrow H^+ + H + He$ (Johnsen and Biondi 1974; and Appendix A).

The high abundance of the neutral molecules CO, OH, and H_2O relative to the various molecular ions reflects the large dissociative recombination rate coefficients. The ratio of OH to H_2O is determined by the photodissociation rate $G(H_2O \rightarrow OH)$ and by the branching ratio $\beta_4(H_3O^+ \rightarrow OH)/\beta_4(H_3O^+ \rightarrow H_2O)$ (eqs. [B6]–[B8]). The large ratio of CO to OH and H_2O, from which CO is formed in this model, is a direct result of the small value adopted in Table 3 for the photodestruction rate $G(CO)$. The maximum abundances relative to O of HCO and CO^+, which have not been plotted in Figure 1, are $\sim 10^{-8}$.

It must be emphasized that the results of Figure 1 represent a local solution of the abundance problem for fixed cloud conditions. One of the most important sources of variation in an actual cloud is the attenuation of the dissociating radiation by dust grains. This attenuation will lead to substantial suppression of the decrease in the ratios $n(X)/n(O)$ with f for large f depicted in Figure 1. To investigate this in more detail, we have included attenuation for the photodestruction rates by the approximate formula,

$$G(X) = G_0(X) \exp\left[-\tau_{gr}(X)\right]. \quad (1)$$

Here $G_0(X)$ is the rate appropriate to a very diffuse cloud, and $\tau_{gr}(X)$ is the mean optical depth for grain attenuation for the radiation band important for the photodissociation of molecule X. The relevant optical depths are given in Table 3. We have also included the variation in f with column density N of hydrogen (in both atomic and molecular form) using results based

on our earlier model calculations for diffuse clouds (Glassgold and Langer 1974), which agree with the OAO-3 results that H_2 becomes abundant ($f \gtrsim 0.1$) for $A_v \gtrsim 0.2$. We continue to assume that n and T are constant. Although these isobaric model calculations support the approximate isothermality of diffuse clouds, the density n does increase with N as atomic hydrogen is converted into molecular form. This effect will require a more detailed model calculation of the type previously reported for H_2.

The results for this schematic cloud model based on equation (1) and on previous calculations for f versus N are illustrated by Figures 2–4. In considering these curves, it should be noted that most of the dramatic variation of f with N due to H_2 self-shielding occurs for $N \lesssim (3\text{–}4) \times 10^{20}$ cm^{-2}, and that f increases rather slowly for larger N. This variation of f implies that the abundance ratios $n(X)/n(O)$ will decrease very rapidly with decreasing N below 3×10^{20} cm^{-2}. The results plotted in Figures 2–4 are column densities $N(X)$ versus N. These curves show the dominance of the decreasing photodissociation rates by attenuation over the decrease in the production rates due to the decrease in H^+ and O^+ abundances. The solid curves in Figure 2 are for the standard run defined by Table 3. The dash curves indicate the effect of changing only the branching ratio $\beta_4(H_3O^+ \rightarrow H_2O)/\beta_4(H_3O^+ \rightarrow OH)$ from 1 to 4. The main effect is to increase the steady-state H_2O abundance. The CO abundance is hardly affected at all; in effect its production is determined by the sum of the OH and H_2O densities rather than their individual values. The OH abundance is also changed very little, since a good fraction of the H_2O molecules formed by dissociative recombination of H_2O are converted into OH by photodissociation. The broken curve with alternating dots and dashes shows $N(CO)$ when $G_0(CO)$ is decreased from 10^{-11} s^{-1} to 3×10^{-12} s^{-1}. For the examples considered in this figure ($N < 10^{21}$ cm^{-2}), photodissociation is the dominant destruction mechanism for CO, so its abundance varies as $n/G_0(CO)$.

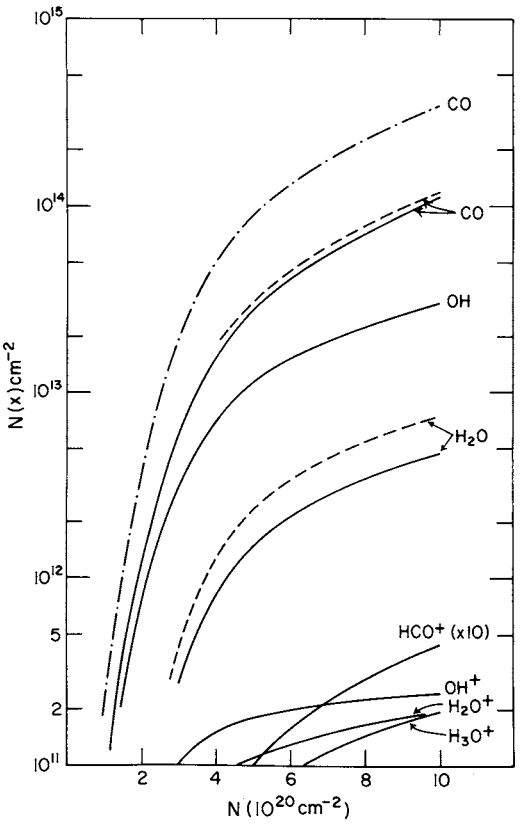

FIG. 2.—Column densities of species X (labeled on curves) as a function of hydrogen column density N into an interstellar cloud. The solid curves are for the "standard" parameters defined in Tables 1–3, and Table A1, and in the text. The dash curve (– – –) indicates the effect of changing the branching ratio $\beta_4(H_2O)/\beta_4(OH)$ from 1 to 4, while the alternating dash curve (–·–·–) indicates the effect of reducing $G(CO)$ to 3×10^{-12} s^{-1}.

The effects of varying ζ_p are illustrated in Figure 3. The solid curves are for the standard run, except that $n = 30$ cm^{-3}. The dash curves indicate that increasing ζ_p from 10^{-17} s^{-1} to 5×10^{-17} s^{-1} leads to an almost linear increase in molecular abundances. This effect can be understood from equation (B10) for O^+ and equation (A8) for H^+, to which it is proportional. In this region $x(H^+)$ depends linearly on the cosmic-ray ionization rate ζ_p and

$$x(O^+) \approx \frac{\zeta'/ne^{-232/T}\xi_O}{\frac{1}{2}fk_8e^{-232/T}\xi_O + \alpha\xi_i},$$

where ξ_i is the abundance of heavy ions with ionization potentials less than 13.6 eV and k_8 is defined in Table 1. In Figure 4 we illustrate the effects of changing temperature. The solid curves are for the standard run, except that $n = 300$ cm^{-3}. The dash curves indicate the effect of reducing the temperature from 80 to 40 K. The marked decrease in molecular abundance can be understood from the above expression for $x(O^+)$. When $\xi_i\alpha \gg \frac{1}{2}fk_8\xi_Oe^{-232/T}$, $x(O^+)$ is a strong function of temperature. For the parameters and rate constants used in this paper, we expect this T dependence to be most important for $T \lesssim 50$ K. Figures 2–4 also demonstrate the dependence on density of the abundances of CO, OH, and H_2O. At larger column densities the OH and H_2O abundances and column densities are relatively insensitive to n. This insensitivity can be understood from the density dependence of $x(O^+)$, which essentially gives the production rate of OH and H_2O, and the destruction rate $g(X) = G(X)/n$. The abundance formulae of Appendix B and the above expression for $x(O^+)$ imply, for example, that $x(OH) \approx x(O^+)/g(OH)$ so that the $1/n$ dependence in $g(OH) = G(OH)/n$ cancels that in $x(O^+)$. The CO abundance is proportional to $x(C^+)$ and to $x(OH) + x(H_2O)$ (which are all independent of n), but its destruction rate is still inversely proportional to n so that $x(CO) \propto n$. The CO curves in Figures 2–4 reflect this dependence.

To conclude this section we should note that the major limitation in the way in which we have used the balance equations to obtain the abundances of CO,

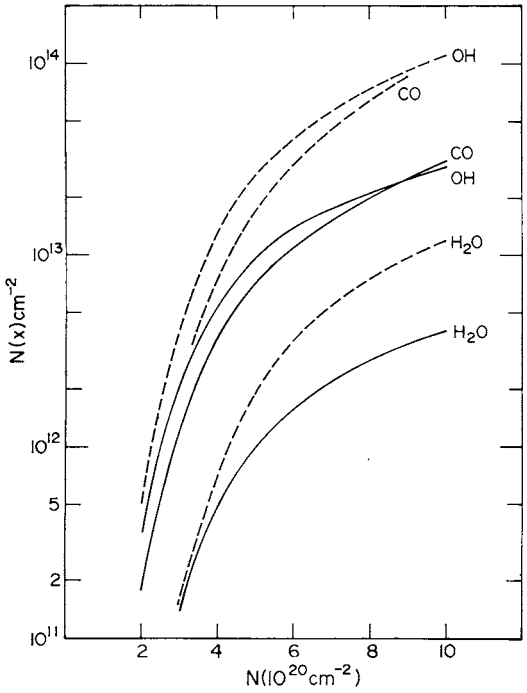

FIG. 3.—Column densities for the neutral molecules as a function of hydrogen column density into an interstellar cloud. The curves are for $n = 30\ \mathrm{cm}^{-3}$ and $G(\mathrm{CO}) = 10^{-11}\ \mathrm{s}^{-1}$; otherwise the "standard" parameters defined in Tables 1–3 and Table A1 are used. The dash curves indicate the effect of increasing ζ_p to $5 \times 10^{-17}\ \mathrm{s}^{-1}$.

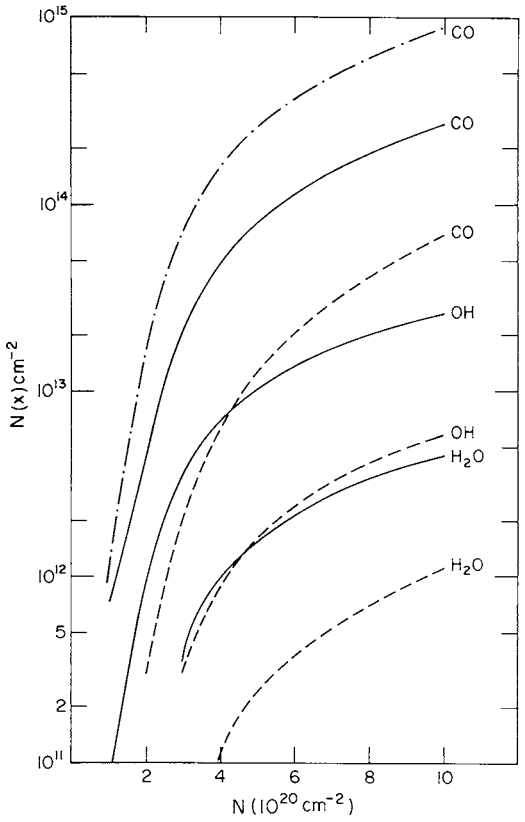

FIG. 4.—Column densities for the neutral molecules as a function of hydrogen column density into an interstellar cloud. The solid curves are for the "standard" parameters defined by Tables 1–3 and Table A1, except that $n = 300\ \mathrm{cm}^{-3}$. The dash curves indicate the effect of decreasing T to 40 K. The alternating dash curve (–·–·–) indicates the effect of decreasing $G(\mathrm{CO})$ to $3 \times 10^{-12}\ \mathrm{s}^{-1}$ (for $T = 80$ K).

OH, H_2O, and related molecules in Figures 1–4, is the tacit assumption that most of the gaseous oxygen and carbon are in the form of O and C^+, rather than in molecules. This assumption means that our results apply only to diffuse or moderately thick clouds in which the column density to the center $N \lesssim (2\text{–}3) \times 10^{21}\ \mathrm{cm}^{-2}$. However, the balance equations in Appendix B will still hold in thicker clouds as long as they are supplemented by appropriate conservation equations for all forms of oxygen and carbon. When this is done, it becomes possible to extend the gas phase abundance theory of oxygen-bearing molecules up to $N \approx 5 \times 10^{21}\ \mathrm{cm}^{-2}$, and to describe the transition from C^+ to CO in warm clouds (Glassgold and Langer 1975). On the basis of the results of this extended theory, it is possible to establish the limits of application of the present results to $N \lesssim 2 \times 10^{21}\ \mathrm{cm}^{-2}$ to the center of a cloud.

III. DISCUSSION

In this concluding section we discuss the relevance of the above calculations to observations. Column densities for CO in diffuse clouds have been measured by Smith and Stecher (1971), Jenkins *et al.* (1973), Morton (1975), Solomon (1974), and Snow (1975). The most recent results for ζ Oph (Morton 1975) give $N(\mathrm{CO}) = 10^{15}\ \mathrm{cm}^{-2}$ to within a factor of 2, whereas Jenkins *et al.* (1973) obtained $4.6 \times 10^{14}\ \mathrm{cm}^{-2}$ for ζ Oph and 1.9, 3.1, and $3.5 \times 10^{13}\ \mathrm{cm}^{-2}$, respectively, for λ Ori, ξ Per, and α Cam. Snow (1975) has found $N(\mathrm{CO}) = (5\text{–}9) \times 10^{14}\ \mathrm{cm}^{-2}$ for o Per and a possible observation of OH with $N(\mathrm{OH}) = (0.7\text{–}1.2) \times 10^{13}\ \mathrm{cm}^{-2}$. Attempts to measure $N(\mathrm{OH})$ toward ζ Oph in the visible (Herbig 1968), ultraviolet (Jenkins *et al.* 1974; Morton 1975), and radio (Turner 1974) have been unsuccessful; Herbig gave an upper limit of $8.3 \times 10^{13}\ \mathrm{cm}^{-2}$. The water molecule has not been observed in diffuse clouds; Snow (1975) reports an upper bound of $10^{12}\ \mathrm{cm}^{-2}$ in o Per. Uncertainties in interpreting the ultraviolet measurements of OH and H_2O arise because the f-values for the relevant transitions are not known but are only estimated.

We attempt a preliminary comparison of the observational information for ζ Oph and o Per by using a slab model in which the hydrogen column densities to the center are $N = 6.8 \times 10^{20}\ \mathrm{cm}^{-2}$ (Morton 1975) and $7.5 \times 10^{20}\ \mathrm{cm}^{-2}$ (Snow 1975), respectively, i.e., one-half the measured values. Referring to the standard run in Figure 2, we see that the corresponding total molecular column densities through the cloud are as follows: $N_t(\mathrm{CO}) \approx 1 \times 10^{14}\ \mathrm{cm}^{-2}$, $N_t(\mathrm{OH}) \approx 4 \times 10^{13}\ \mathrm{cm}^{-2}$, and $N_t(\mathrm{H_2O}) \approx 6 \times 10^{12}\ \mathrm{cm}^{-2}$. (These

values are *twice* those given by the curves for $N = 7 \times 10^{20}$ cm^{-2} because N corresponds to just one-half of the absorbing region in a slab model.) Somewhat fortuitously, the values for N(OH) and $N(H_2O)$ agree roughly with the observations within the experimental uncertainties. If we take into account the latitude in the theoretical calculations, it would not be difficult to get good agreement with the smaller observational values. For example, if $G_0(OH) \approx 5 \times 10^{-10}$ s^{-1} were chosen instead of the value in the standard parameter set, almost exact agreement would be obtained. The CO abundances are, however, not in agreement, being too small by a factor of 5–10; the disagreement increases if ζ_p and G(OH) are adjusted to give smaller values of N(OH). However, Figures 2 and 4 indicate how this difficulty can easily be resolved by using a smaller dissociation rate, $G_0(CO) = 3 \times 10^{-12}$ s^{-1} (Fig. 2), and/or a higher density n. As discussed earlier, changing n (for $n \gtrsim 50$ cm^{-3}) hardly affects the OH abundance but does change x(CO). In evaluating the significance of this comparison, one must bear in mind the crudity of a slab model and the sensitivity to rate constants, as exemplified by Figures 2–4. Referring again to these figures, we see that changing ζ_p and T affects all three neutral oxygen-bearing molecules similarly; changing G(CO) affects only CO, and varying $G(H_2O)$ and $\beta_4(H_3O^+ \rightarrow H_2O)/\beta_4(H_3O^+ \rightarrow OH)$ alters the H_2O/OH ratio.

One reason why the standard run cannot be compared directly with ζ Oph and o Per measurements is that the ultraviolet attenuation by grains has been calculated for a typical star rather than for these particular ones. According to far-ultraviolet selective-extinction measurements with OAO-2 (Bless and Savage 1972) and OAO-3 (York *et al.* 1973), grain attenuation in the direction of ζ Oph increases more rapidly with decreasing wavelength than for the typical reddened star. Assuming an albedo of unity, we have transcribed these measurements into frequency-dependent grain absorption cross sections per gas atom (Fig. 1*a*, Glassgold and Langer 1974). The optical depths τ_{gr}(CO) and τ_{gr}(OH) may then be calculated for a given value of N by averaging the grain cross sections over the photodissociation probabilities for CO and OH. According to the discussion in § II, little is known about these probabilities, and so we have obtained τ_{gr}(CO) and τ_{gr}(OH) by using grain cross sections at characteristic wavelengths, 1000 Å for CO and 1100 Å for OH. Thus we estimate for ζ Oph (and possibly o Per): $\tau_{gr}(CO) \approx N/(5 \times 10^{20}$ cm$^{-2})$ and $\tau_{gr}(OH) \approx N/(8 \times 10^{20}$ cm$^{-2})$, respectively 60 percent and 25 percent larger than the values given in Table 3 for the typical reddened star. All other things being equal, these changes imply increases in the local abundance of CO and OH in the middle of these clouds by ~100 percent and ~25 percent, respectively. Furthermore, the CO abundance is proportional to ξ_C, and uncertainties in the depletion of carbon have a direct effect on our estimates. The abundance of oxygen is less important because, as previously discussed, the OH and H_2O abundances are insensitive to ξ_O for warm clouds.

It has been suggested that the absorbing clouds in front of both ζ Oph (Black and Dalgarno 1973*a*) and o Per (Snow 1975) have densities $n \approx 1000$ cm^{-3}, and radiation field intensities considerably larger than the average. For illustrative purposes we consider the effect of the o Per cloud of scaling the density and radiation field by a factor of 3 from the results at $n = 300$ cm^{-3} [i.e., $n' \approx 900$ and $G'(X) \approx 3G(X)$]. Referring to Figure 4, we find that the calculated OH and CO column densities become $N_t(OH) \approx 3 \times 10^{13}$ cm^{-2}, $N(CO) \approx 3 \times 10^{14}$ cm^{-2} for the larger value of G(CO), and $N(CO) \approx 1.1 \times 10^{15}$ cm^{-2} for the smaller value. When $N \lesssim 4 \times 10^{21}$ cm^{-2} and x(OH) $\gg x(H_2O)$, this result can be expressed simply in terms of the CO to OH ratio (from eq. [B14]),

$$\frac{x(CO)}{x(OH)} \approx \frac{k' x(C^+)}{g_0(CO) \exp[-\tau_{gr}(CO)] + k_{25} x(He^+)}, \quad (2)$$

where $k' \approx k_{17} + k_{18} \approx k_{19} + k_{20}$. For diffuse clouds with 3×10^{20} cm$^{-2} < N < 1 \times 10^{21}$ cm^{-2}, the attenuation factor dominates the variation of this ratio through the cloud. Equation (2) can be used to estimate the density from measured CO/OH ratios when $F \gtrsim 0.25$, where $F \equiv 2N(H_2)/N$:

$$n \approx 5 \times 10^3 [G(CO)/10^{-11}] \times \exp[-\tau_{gr}(CO)][N(CO)/N(OH)] \text{ cm}^{-3}.$$

Very recently Crutcher and Watson (1976) have observed OH at 3078 Å toward ζ Oph and o Per, with column densities $N(OH) = 3 \times 10^{13}$ cm^{-2} and 1.0×10^{14} cm^{-2}, respectively. In accord with the above discussion, it is not difficult to obtain agreement between these measurements and the present calculations.

The measured CO column densities for λ Ori, α Cam, and ξ Per are smaller than those for ζ Oph and o Per by factors roughly between 30 and 50. The predictions of our standard run are too large for these clouds. Comparison of theoretical predictions for different clouds is always difficult because of the many possible differences in physical properties. We have already indicated how some of the more sensitive model parameters affect the calculated molecular column densities. For the ζ Oph and o Per clouds, it was necessary to consider densities much higher than the value $n = 100$ cm^{-3} adopted in our standard run. The determination of density is significant because $x(CO) \propto n$. Thus the use of lower densities in the range 10–30 cm^{-3}, typical of some diffuse clouds, may explain the CO measurements for α Cam, ξ Per, and λ Ori. (See, for example, the curves in Fig. 3.) Furthermore, at smaller column densities the results will be sensitive to variations of f with n and N, which are dependent on the specific cloud models used in a calculation.

Sancisi *et al.* (1974) have obtained OH column densities from emission line measurements in the radio for the large dust cloud in the region of the Perseus

OB2 association. They have plotted $N(\mathrm{OH})$ versus N for $0.3 \lesssim N \lesssim 2.5$, obtaining N from extinction determinations based on star counts. Although their plot shows considerable scatter, a threshold behavior is found characterized by a total column density $N_t \approx 6 \times 10^{20}\ \mathrm{cm}^{-2}$. This threshold is consistent with the requirements of the present gas-phase ion-molecule basis for OH production, because a substantial fraction of H_2 is not obtained until $N_t \approx 2\text{–}4 \times 10^{20}\ \mathrm{cm}^{-2}$. Sancisi *et al.* also found that $N_t(\mathrm{OH})$ increases from $3 \times 10^{13}\ \mathrm{cm}^{-2}$ to $\sim 10^{14}\ \mathrm{cm}^{-2}$ as N_t varies from $6 \times 10^{20}\ \mathrm{cm}^{-2}$ to $2 \times 10^{21}\ \mathrm{cm}^{-2}$, consistent with the results plotted in Figures 2 and 4.

Upper limits have been placed on the column density of CO^+ in diffuse clouds by Herbig (1968), Jenkins *et al.* (1973), and Hobbs (1973); typical values are $\sim 10^{13}\ \mathrm{cm}^{-2}$. Our calculated values are consistent with this result, but so much smaller that little significance can be attached to the comparison. The recent confirmation that X-ogen is HCO^+ (Snyder 1975) has little bearing on the calculations of HCO^+ in this paper on diffuse clouds. The radio observations of HCO^+ are generally made on considerably thicker clouds than discussed in this paper. We have introduced a new production mechanism for the formyl radical HCO, $C^+ + H_2O \rightarrow HCO + H^+$, in the above calculations (reaction 20). This radical has recently been detected by Hollis, Snyder, and Ulich (1975) in clouds thicker than considered here. Although there are other reactions important for the HCO abundance in such clouds, we believe that the above reaction makes an important contribution. Further discussion of the HCO^+ and HCO abundances will be given in a forthcoming paper (Langer 1976*b*).

In conclusion, this preliminary comparison of the abundance calculations with the limited observational information on oxygen-bearing molecules in diffuse clouds indicates that the present model is in reasonable agreement with the experimental data. The theory can therefore be made the basis for more detailed analysis of the observations.

Since the first version of this article was completed in the early summer of 1974, the authors have greatly benefited from many comments from colleagues (including referees), too numerous to acknowledge in detail. We are especially appreciative, however, of conversations with E. E. Ferguson on He^+ charge exchange, M. A. Biondi on the $He^+ + H_2$ dissociative charge exchange reaction, and William H. Smith on OH photodissociation. In addition, we have benefited from discussions with and/or communications of unpublished observational results from D. C. Morton, T. P. Snow, P. Solomon, P. Thaddeus, and B. Turner. One of us (W. D. L.) wishes to acknowledge support as an NRC-NAS Senior Associate during the completion of this research.

This work has been supported by grant NGR-33-016-196 from the National Aeronautics and Space Administration.

APPENDIX A

The densities of electrons and ions play an important role in determining the physical and chemical properties of interstellar clouds. In this Appendix we extend the theory of ionization of interstellar clouds to moderately thick clouds (column densities through the cloud $N_t \lesssim 4 \times 10^{21}\ \mathrm{cm}^{-2}$). This work is a continuation of an earlier discussion of ionization in diffuse clouds (Glassgold and Langer 1974*a*, especially Appendix A), which dealt mainly with the effective cosmic-ray ionization rates for mixtures of H, H_2, and He. The major applications of the present work are to the abundances of oxygen-bearing molecules and to the He^+/H^+ ratio.

There are two main sources of electrons in interstellar clouds: ionization by the radiation field of heavy elements with ionization potentials $I < 13.6$ eV (e.g., carbon), and cosmic-ray ionization of atomic and molecular hydrogen and helium. In the outermost parts of clouds, X-rays also contribute to photoionization, with an estimated ionization rate $\zeta_x \approx 2 \times 10^{-16}\ \mathrm{s}^{-1}$ arising mainly from 0.1–0.2 keV photons. We neglect this contribution because the optical depth for 0.1 keV X-rays, $\tau_x \approx N/(2 \times 10^{19}\ \mathrm{cm}^{-2})$, is large for the regions of interest in this paper ($N \gtrsim 2 \times 10^{20}\ \mathrm{cm}^{-2}$).

Field and Steigman (1971) pointed out that charge exchange of H^+ with atomic oxygen is important in determining the ionization of the interstellar medium. As discussed in the text, when molecular hydrogen is present in interstellar clouds, the O^+ produced by charge exchange interacts with H_2 to form OH^+, and in subsequent interactions with H_2 and electrons a variety of oxygen-bearing molecules and molecular ions are formed. The primary effect of these reactions is to remove H^+ and electrons at a greater rate than if only radiative recombination were operative. The estimated rate (as discussed in the text) depends sensitively on temperature because $H^+ + O$ charge exchange is endothermic by 232 K. Some of the molecules formed from the chain beginning with O^+—namely, OH and H_2O—can charge exchange exothermically with H^+ and He^+. Their effect on the ionization balance can be neglected, however, when $T > 50$ K if $[n(\mathrm{OH}) + n(H_2O)]/n(\mathrm{O}) < 10^{-2}$.

We include a reaction which has not been previously considered in problems of this type, dissociative charge exchange of He^+ and H_2,

$$He^+ + H_2 \rightarrow H + H^+ + He\,. \qquad \text{(A1)}$$

The rate constant for this reaction has recently been measured by Johnsen and Biondi (1974) to be $\approx 10^{-13}\ \mathrm{cm}^3\ \mathrm{s}^{-1}$ at 300 K. Despite this small value, reaction (A1) is an important source of H^+ when the fractional abundance of H_2 is high ($f > 0.9$), and it can dominate the recombination of He^+ even for small values of f (~ 0.1).

The He^+/H^+ ratio in H I regions has been discussed by Jura and Dalgarno (1971), but when H_2 is present, even in small amounts ($f \approx 0.1$), their analysis does not apply because reaction (A1) is important. Furthermore, if $T \gtrsim 40$ K the $H^+ + O$ charge exchange must be included. Brown and Gómez-González (1974) considered the effect of charge exchange on the He^+/H^+ ratio in diffuse clouds containing H_2, but not $He^+ + H_2$ dissociative charge exchange. Their He^+ abundances are likely to be too large, and for H^+ at large f too small. Furthermore, the extension of their treatment to dark clouds is probably not valid, since they neglect charge exchange with some other molecules, e.g., OH, H_2O, and CO.

The H^+ ion can also charge exchange with deuterium ($D + H^+ \rightarrow H + D^+$) (Black and Dalgarno 1973*a*; Watson 1973*a*), but this does not lead to a significant reduction in $n(H^+)$ because D^+ reacts rapidly with H and H_2 to produce H^+ again ($D^+ + H \rightarrow H^+ + D$ and $D^+ + H_2 \rightarrow HD + H^+$). The HD density, which we will discuss briefly below, can be used to estimate the primary cosmic-ray ionization rate on hydrogen, ζ_p, through its connection to H^+ via these reactions (Black and Dalgarno 1973*a*; Jura 1974; O'Donnell and Watson 1974).

The electron and ion densities influence the physical properties of interstellar clouds in numerous ways. For example, as discussed in the text, the H^+ ion is important for the formation of molecules other than HD. The He^+ ion is significant because He^+ can destroy CO by dissociative ionization. The electron density is important because it is basic to the thermal balance of the cloud, since electrons collisionally excite and de-excite cooling transitions.

The electron and ion abundances will be determined by solving the chemical balance equations for all the constituents using the constraints of charge neutrality and conservation of number density for each nuclear species. The problem is complex, but it can be solved approximately in a number of different limits. We restrict ourselves to a regime characteristic of many of the clouds which have recently come under study—namely, diffuse to moderately thick clouds $0.1 < A_v \lesssim 2$ with densities $n \lesssim 10^3$ cm^{-3}. These clouds are relatively warm ($50 \lesssim T \lesssim 100$ K) and contain substantial amounts of molecular hydrogen ($f \gtrsim 0.1$). The H_2 column densities in diffuse clouds (Spitzer *et al.* 1973) indicate that locally $f = 0.1$ is reached when the total hydrogen density into the cloud, $N = N(H) + 2N(H_2)$, becomes $\gtrsim 2.5 \times 10^{20}$ cm^{-2}. This result is supported by theoretical studies (Hollenbach, Werner, and Salpeter 1971; Glassgold and Langer 1973*a*, 1974; Jura 1974). Kinetic temperatures in the range 60–120 K have been determined for these clouds from the relative populations of the lowest $J = 0$ and 1 states of H_2 (Spitzer and Cochran 1973; Spitzer, Cochran, and Hirshfeld 1974). The temperatures in somewhat thicker clouds may be lower, e.g., because of the attenuation of external heating radiations. Thus we are interested in determining the electron and ion abundances in regions where the interstellar gas is predominantly a mixture of He, H, and H_2 with $f \geq 0.1$, where $40 \lesssim T \lesssim 100$ K, and where cosmic rays make some contribution to the ionization rate. The results in this paper are also restricted to clouds where $N \lesssim 2 \times 10^{21}$ cm^{-2} to the center, because for thicker clouds the abundance of CO, OH, and H_2O can become large enough to make a significant effect on the ion balance equations (Glassgold and Langer 1975).

We list the main reactions which determine the electron and ion abundances in the clouds under consideration in Table A1. The rates for cosmic-ray ionization of H, H_2, and He, including direct ionization by the cosmic rays and ionization by secondary electrons, have been discussed previously (Glassgold and Langer 1973, 1974). The branching ratio for dissociative ionization of H_2 by cosmic rays ($p + H_2 \rightarrow H + H^+ + e + p$) in Table A1 is less than half that used by Solomon and Werner (1971). The present value, based on experiments by Adamczyk *et al.* (1966), is preferable for cosmic-ray energies ≥ 2 MeV.

The charge exchange reactions produce and/or destroy the ions H^+, D^+, and O^+. The ion-molecule reactions which make H_3^+, HD, and OH^+ are listed next; OH^+ subsequently reacts to form other oxygen-bearing molecules and molecular ions. For the regions under discussion in this paper the dissociative charge exchange reaction of He^+ with H_2 dominates over other H^+-producing reactions with molecules because the large abundance of H_2 more than compensates for the small rate constant k_9. Thus the fast reaction $C^+ + OH \rightarrow CO + H^+$ (Herbst and Klemperer 1973; O'Donnell and Watson 1974) cannot compete with k_9 until the fractional abundance of OH becomes as large as $10^{-4}x(He^+)/x(C^+)$, where $x(He^+)$ and $x(C^+)$ are the fractional abundances of He^+ and C^+. For diffuse and moderately thick clouds this would require $x(OH) \approx 10^{-5}$, but this large an abundance may not be achieved until $N \gtrsim 10^{22}$ cm^{-2}. Similar considerations apply to other sources of H^+ such as $CH^+ + O \rightarrow CO + H^+$, and we neglect them here. Dalgarno, Oppenheimer, and Berry (1973) have suggested that chemi-ionization by $CH + O \rightarrow HCO^+ + e$ (rate constant 10^{-11}–10^{-10} cm^3 s^{-1}) could be an important source of electrons in interstellar clouds. In the regions of interest here this source is not important because of the low abundance of CH, $x(CH) \ll 10^{-7}$. Finally, Jura (1974*a*) has suggested that photodestruction of HCl^+ ($h\nu + HCl^+ \rightarrow H^+ + Cl$) is a source of H^+. The rate of H^+ production from HCl^+, $\zeta(HCl^+) = G_d(HCl^+)x(HCl^+) \approx 3 \times 10^{-16} f[(1 + 3f/n)(f + 3/n)]^{-1}$, is $\sim 2 \times 10^{-17}$ s^{-1} for $f = 0.1$ and $n = 10$, comparable with cosmic-ray production of H^+ when $\zeta_p = 10^{-17}$ s^{-1}. With increasing f and $n > 10$ cm^{-3}, $\zeta(HCl^+) \approx 10^{-16}/n$ s^{-1}, and therefore HCl^+ production of H^+ can be ignored in this work.

We have also omitted other H^+-destroying charge exchange reactions with neutral molecules because the relevant molecular abundances are too small in the clouds under consideration. For example, the rate constants for $H^+ + OH \rightarrow H + OH^+$ and $H^+ + H_2O \rightarrow H + H_2O^+$ are probably $\sim 10^{-9}$ cm^3 s^{-1}, but these reactions destroy H^+ at a rate 10–100 times slower than does charge exchange with O for temperatures in the range 40–100 K since $x(OH + H_2O) \ll 10^{-2}$. The densities of oxygen-bearing molecular ions such as OH^+, H_2O^+, and H_3O^+

TABLE A1

PRIMARY REACTIONS

Reaction	Rate*	Reference
Cosmic-Ray Ionization		
$p + H \rightarrow H^+ + e + p$	$\zeta_1 = 1.5\zeta_p$	1
$p + H_2 \rightarrow H_2^+ + e + p$	$\zeta_2(H_2^+) = 2.3\zeta_p$	1
$p + H_2 \rightarrow H + H^+ + e + p$	$\zeta_2(H^+) = 0.022\zeta_2(H_2^+)$	1
$p + He \rightarrow He^+ + e + p$	$\zeta(He) = 1.5\zeta_p$	1
Charge Exchange		
$H_2^+ + H \rightarrow H_2 + H^+$	$k_1 = 6 \times 10^{-10}$	2
$D + H^+ \rightarrow D^+ + H$	$k_3 = 2 \times 10^{-9} e^{-43/T}$	3
$D^+ + H \rightarrow D + H^+$	$k_4 = 2 \times 10^{-9}$	3
$O + H^+ \rightarrow O^+ + H$	$k_5 = 10^{-9} e^{-232/T}$	4
$O^+ + H \rightarrow O + H^+$	$k_6 = 10^{-9}$	4
Ion-Molecule Reactions		
$H_2^+ + H_2 \rightarrow H_3^+ + H$	$k_2 = 2 \times 10^{-9}$	5
$D^+ + H_2 \rightarrow HD + H^+$	$k_7 = 10^{-9}$	6
$O^+ + H_2 \rightarrow OH^+ + H$	$k_8 = 1.6 \times 10^{-9}$	7
Dissociative Charge Exchange		
$He^+ + H_2 \rightarrow He + H + H^+$	$k_9 = 10^{-13}$	8
Radiative and Dissociative Recombination		
$e + H^+ \rightarrow H + \gamma$	$\alpha(H^+) = 1.9 \times 10^{-10} T^{-0.7}$	9
$e + He^+ \rightarrow He + \gamma$	$\alpha(He^+) = \alpha(H^+)$	9
$e + H_3^+ \rightarrow 3H$ or $H_2 + H$	$\beta_1(H_3^+) = 4 \times 10^{-6} T^{-0.5}$	10

REFERENCES.—
1. Glassgold and Langer 1973.
2. de Jong 1972.
3. Smith 1966.
4. Field and Steigman 1971.
5. Neynaber and Trujillo 1972.
6. Fehsenfeld *et al.* 1973.
7. Kim, Theard, and Huntress 1975.
8. Johnsen and Biondi 1974.
9. Spitzer 1968.
10. Leu, Johnson, and Biondi 1973.

* All rates are in units of $cm^3\ s^{-1}$ unless otherwise noted.

are negligible compared with the total ion density. Charge exchange and other ion-molecule reactions initiated by other atomic ions such as C^+, He^+, etc., can be ignored for similar reasons.

The chemical balance equations yield the following relationships for the fractional abundance, $x(i) = n(i)/n$, of the ions:

$$x(He^+) = \frac{\xi_{He}\zeta(He)/n}{\alpha(He^+)x_e + k_9 f/2}, \tag{A2}$$

$$x(O^+) = \frac{2k_5\xi_O x(H^+)}{2k_6 + (k_8 - 2k_6)f}, \tag{A3}$$

$$x(H^+) = \frac{\zeta_H/n + \frac{1}{2}fk_9 x(He^+)}{\alpha(H^+)x_e + C}, \tag{A4}$$

$$\zeta_H = \left[\zeta_1 + \frac{k_1 f\zeta_2(H_2^+)}{2k_1 + (k_2 - 2k_1)f}\right](1 - f) + \zeta_2(H_2^+)f/2,$$

$$C = \frac{k_8 f k_5 \xi_O}{2k_6 + (k_8 - 2k_6)f},$$

$$x(H_3^+) = \frac{k_2 f^2 \zeta_2(H_2^+)/n}{2\beta_1(H_3^+)x_e[2k_1 + (k_2 - 2k_1)f]}, \tag{A5}$$

where ξ_{He} and ξ_O are fractional abundances relative to hydrogen. Thus we have anticipated the conclusions implied by equations (A2) and (A3), that He and O are mainly neutral for the clouds under consideration. On the other hand, we take the elements with $I < 13.6$ eV to be predominantly ionized. If ξ_i is the total relative abundance of these elements, charge conservation implies

$$x_e = \xi_i + x(H^+) + x(He^+) . \tag{A6}$$

The relative abundances of H_2^+ and H_3^+, as well as all other atomic and molecular ions, are too small ($< 10^{-6}$) to be included in equation (A6).

When He^+ radiative recombination can be ignored ($\alpha x_e \ll k_9 f/2$ in eq. [A2]), $x(He^+)$ is independent of x_e, and we can solve the ion abundances analytically [also assuming $\alpha(He^+) \approx \alpha(H^+) = \alpha$]. If we use the values for α and k_9 in Table A1, the condition for ignoring radiative recombination of He^+ is $f \gg 200 x_e$ for temperatures in the range from 40–100 K. Because x_e is roughly of the order of 10^{-4} provided $\zeta_p \leqslant 10^{-16}$ s^{-1}, this condition is fulfilled as soon as a moderate fraction of hydrogen has been converted to molecular form, say $f \approx 0.1$. Moreover, the following approximation is appropriate when $x(He^+) \ll \zeta'/(nC)$,

$$x_e \approx \tfrac{1}{2}\{(\xi_i - C/\alpha) + [(\xi_i + C/\alpha)^2 + 4\zeta'/n\alpha]^{1/2}\} , \tag{A7}$$

$$x(H^+) = \tfrac{1}{2}\{-(\xi_i + C/\alpha) + [(\xi_i + C/\alpha)^2 + 4\zeta'/n\alpha]^{1/2}\} , \tag{A8}$$

where $\zeta' = \zeta_H + \xi_{He}\zeta_{He}$. Equations (A7) and (A8) work well over the range of parameters considered in this work.

Electron and ion abundances are plotted in Figure 5 as a function of f for a typical parameter set: $n = 100$ cm^{-3}, $\zeta_p = 5 \times 10^{-17}$ s^{-1}, $\xi_O = 2 \times 10^{-4}$, $\xi_i = 7 \times 10^{-5}$ (corresponding to heavy element depletion by a factor of 7), and $\xi_{He} = 1/12$, for two values of temperature, $T = 40$ and 80 K. The He^+ fractional abundance decreases rapidly with f (increasing H_2 abundance) as a result of dissociative charge exchange. The rapid decrease in $x(H^+)$ at

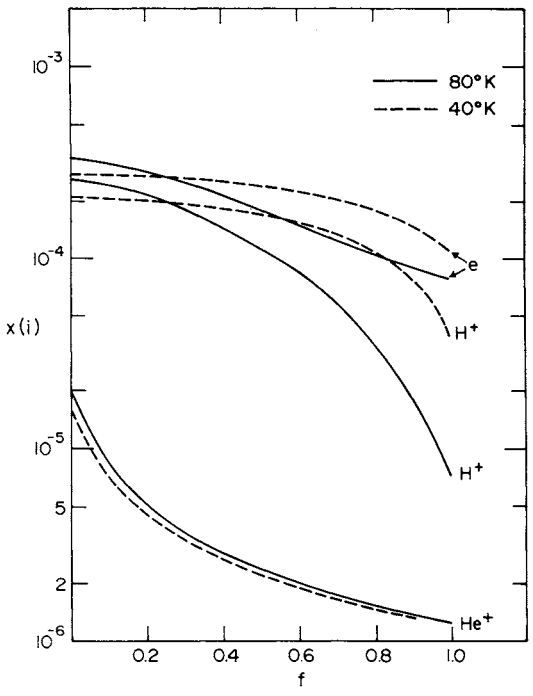

FIG. 5

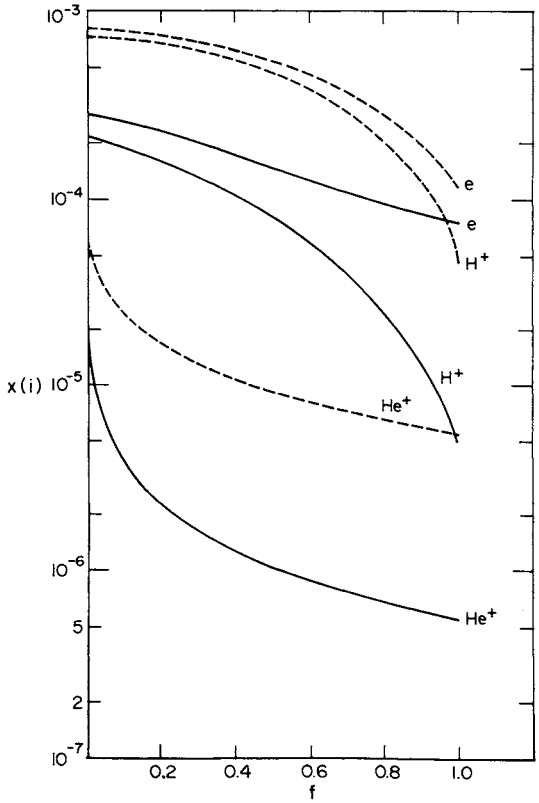

FIG. 6

FIG. 5.—Fractional abundances of electrons, H^+, and He^+ as a function of fractional H_2 abundance $f = 2n(H_2)/n$ for $n = 100$ cm^{-3}, $\zeta_p = 5 \times 10^{-17}$ s^{-1}, $\xi_O = 2 \times 10^{-4}$, $\xi_i = 7 \times 10^{-5}$, $\xi_{He} = 1/12$, and two values of temperature, $T = 40$ and 80 K.

FIG. 6.—Fractional abundances of electrons, H^+, and He^+ as a function of fractional H_2 abundance $f = 2n(H_2)/n$ for $n = 30$ cm^{-3}, $T = 80$ K, $\xi_O = 2 \times 10^{-4}$, $\xi_i = 7 \times 10^{-5}$, $\xi_{He} = 1/12$, and two values of cosmic-ray ionization rate, $\zeta_p = 10^{-17}$ and 10^{-16} s^{-1}.

large f occurs for the following reasons: (i) the disappearance of direct cosmic-ray ionization of H as $f \to 1$ (cf. the first term in ζ_H); (ii) the smallness of dissociative ionization of H_2; and (iii) competition of $O^+ + H_2 \to OH^+ + H$ with $O^+ + H \to O + H^+$. The H^+ abundance depends sensitively on temperature, as is illustrated in Figure 5 by the curve for $T = 40$ K. The changes induced in Figure 5 can be understood from equations (A7) and (A8) in terms of the two most important variables, $\zeta_p/(n\alpha)$ and $C \approx \xi_0 f 10^{-9} e^{-232/T}$ cm^3 s^{-1}. In Figure 6 we indicate some of these changes when $T = 80$ K, but $n = 30$ cm^{-3} and $\zeta_p = 10^{-17}$ s^{-1} and 10^{-16} s^{-1}.

The reduction in the He^+ abundance by dissociative charge exchange with H_2 has implications for the ion-molecule reaction chemistry of the interstellar gas. Herbst and Klemperer (1973) and Watson (1974) emphasized that He^+ is destroyed in dense clouds by dissociative charge exchange with CO (Table 2), whose rate constant is $k_{25} = 1.6 \times 10^{-9}$ cm^3 s^{-1} (Laudenslager, Huntress, and Bowers 1974). In order for this reaction to compete with reaction (A1), the relative CO abundance must be $\sim 2 \times 10^{-5}$. Unless x(CO) is much greater than this value, the He^+ abundance is much smaller than given in previous work.

The theory of the abundance of HD provides a good example of the usefulness of the above results. The main production and destruction mechanisms for this molecule are, respectively, $D^+ + H_2 \to HD + H^+$ and $h\nu + HD \to H + D$ [rate G(HD)]. The balance equations (Black and Dalgarno 1973*a*; Jura 1974; O'Donnell and Watson 1974) can be set up with the aid of the reactions given in Table A1 and the above ion density formulae. We have made comparisons, with measured column density ratios $N(HD)/N(H_2)$ from OAO-3 (Spitzer *et al.* 1973, 1974) using $\xi_D = 1.4 \times 10^{-5}$ (Rogerson and York 1973) and $G_0(HD) = 5 \times 10^{-11}$ s^{-1} (Stephens and Dalgarno 1972; Jura 1974), where G_0 is the dissociation rate at the surface of a cloud. Our conclusion supports those of previous workers (Black and Dalgarno 1973*a*; Jura 1974; O'Donnell and Watson 1974) that ζ_p is likely to lie in the range 10^{-17}–10^{-16} s^{-1}. Though most of the observations suggest the smaller values in this range ($\zeta_p \approx 10^{-17}$ s^{-1}), there are large fluctuations from cloud to cloud, and a quantitative theoretical correlation must still be given. Any estimate of ζ_p based on the HD abundances must be considered to be tentative at this point.

Dissociative charge exchange of He^+ with H_2 is important for the production and destruction of molecules in regions of interstellar clouds with large $f \gtrsim 0.6$. The local f values are always greater than the corresponding column density ratios $F \equiv 2N(H_2)/N$. For example, earlier model calculations (Glassgold and Langer 1973) gave, for the case $n = 50$ cm^{-3}, $T = 70$ K, and $\zeta_p = 10^{-16}$ s^{-1}, $f = 0.7$ for $F = 0.5$, and $f = 0.9$ when $F = 0.7$. These values indicate that many of the effects we describe in this Appendix as being important for moderate to large values of f ($\gtrsim 0.6$) are already present in diffuse clouds, and certainly in thicker clouds. The above calculations of the He^+ abundance in diffuse clouds differs from that obtained from older ideas based solely on radiative recombination by factors as large as 20–35 in the range $f = 0.8$–1.0. (This will depend somewhat on the assumed depletion.) Dissociative charge exchange of He^+ with H_2 does not affect the H^+ abundance (and the abundances of D^+, HD, and oxygen-bearing molecules) very much until $f \gtrsim 0.9$. Several of the clouds observed by the Princeton ultraviolet spectrometer on OAO-3 probably have $f \gtrsim 0.8$ in their interior regions, e.g., ζ Oph, ζ Per, and ξ Per (Spitzer *et al.* 1973), and larger values would certainly occur in the thicker and denser clouds.

APPENDIX B

The results of the steady-state balance equations for the molecules and molecular ions containing at least one carbon or oxygen atom are listed below. The reactions are listed in Tables 1 and 2 using the following notation: $g(x) = G(x)/n$, $f = 2n(H_2)/n$, $x_e = n_e/n$, $x(H^+) = n(H^+)/n$, etc., with $n = n(H) + 2n(H_2)$. The species standing at the left indicates which balance equation has been used.

H_3O^+:
$$\frac{x(H_2O^+)}{x(H_3O^+)} = \frac{\beta_4}{k_{16}} \frac{2x_e}{f}, \tag{B1}$$

H_2O:
$$\frac{x(H_3O^+)}{x(H_2O)} = \frac{g(H_2O)}{\beta_4(H_3O^+ \to H_2O)x_e} + \frac{k_{13}x(H^+) + (k_{19} + k_{20})x(C^+)}{\beta_4(H_3O^+ \to H_2O)x_e}, \tag{B2}$$

H_2O^+:
$$\frac{x(OH^+)}{x(H_2O)} = A \frac{g(H_2O) + \bar{k}(H_2O)x_e}{\frac{1}{2}fk_{15}}, \tag{B3}$$

$$A \equiv \frac{\beta_4(H_3O^+)}{\beta_4(H_3O^+ \to H_2O)} \left(1 + \frac{\beta_3(H_2O^+)}{k_{16}} \frac{2x_e}{f}\right), \tag{B4}$$

$$\bar{k}(H_2O) \equiv (k_{19} + k_{20}) \frac{x(C^+)}{x_e} + \frac{A - 1}{A} k_{13} \frac{x(H^+)}{x_e}, \tag{B5}$$

OH:
$$\frac{x(OH)}{x(H_2O)} = B \frac{(1 + b/B)g(H_2O) + [(k_{19} + k_{20})x(C^+) + k_{13}x(H^+)]}{g(OH) + [(k_{17} + k_{18})x(C^+) + k_{10}x(H^+)]}, \tag{B6}$$

$$B = \frac{\beta_4(H_3O^+ \to OH)}{\beta_4(H_3O^+ \to H_2O)}\left(1 + \frac{\beta_3(H_2O^+ \to OH)}{\beta_4(H_3O^+ \to OH)}\frac{\beta_4(H_3O^+)}{k_{16}}\frac{2x_e}{f}\right), \tag{B7}$$

$$b = \frac{g(H_2O \to OH)}{g(H_2O)}, \tag{B8}$$

OH^+:
$$\frac{x(OH^+)}{x(O^+)} = \frac{k_8}{k_{15} + \beta_2(OH^+)2x_e/f}(1 - c)^{-1}, \tag{B9}$$

$$c \equiv \frac{g_i(OH) + k_{10}x(H^+)}{k_{15}f/2 + \beta_2(OH^+)x_e}\frac{x(OH)}{x(H_2O)}\frac{x(H_2O)}{x(OH^+)},$$

O^+:
$$\frac{x(O^+)}{x(O)} = \frac{k_5}{k_6 + (k_8/2 - k_6)f}x(H^+), \tag{B10}$$

HCO^+:
$$\frac{x(HCO^+)}{x(C^+)} = \frac{k_{17}'x(OH) + k_{19}x(H_2O)}{\beta_6(HCO^+)x_e}, \tag{B11}$$

$$k_{17}' = \frac{k_{24}f/2}{k_{23} + (k_{24}/2 - k_{23})f + \beta_5 x_e}k_{17},$$

HCO:
$$\frac{x(HCO)}{x(H_2O)} = \frac{k_{20}x(C^+)}{g(HCO)}, \tag{B12}$$

CO:
$$\frac{x(CO^+)}{x(C^+)} = \frac{k_{17}x(OH)}{k_{23} + (k_{24}/2 - k_{23})f + \beta_5(CO^+)x_e}, \tag{B13}$$

CO:
$$\frac{x(CO)}{x(C^+)} = \frac{(k_{17}'' + k_{18})x(OH) + (k_{19}' + k_{20})x(H_2O)}{k_{25}x(He^+) + g(CO)}, \tag{B14}$$

$$k_{17}'' = \frac{k_{23} + (\frac{1}{2}k_{24}\beta_6(HCO^+ \to CO)/\beta_6 - k_{23})f}{k_{23} + (\frac{1}{2}k_{24} - k_{23})f + \beta_5 x_e}k_{17},$$

$$k_{19}' = \frac{\beta_6(HCO^+ \to CO)}{\beta_6}k_{19}.$$

In deriving the above equations, a certain amount of algebraic manipulation was performed, notably on the ratios $n(OH^+)/n(H_2O)$. In the process it became clear that a few additional approximations were justified for diffuse clouds on the basis of the rate constants given in Tables 1 and 2. For example, $g_i(H_2O)$ was ignored relative to $g(H_2O)$ in equation (B3), and He^+ charge-exchange and ion-molecule reactions with OH and H_2O were ignored in the presence of similar reactions with H^+ and C^+, simply because of the relatively low abundance of He^+. Furthermore, all charge exchange and ion-molecule reactions have been ignored as destruction mechanisms for HCO in the presence of the large photodissociation rate. In conjunction with the specific cases plotted in the figures in the main body of the text these equations can be used to estimate abundance variations with changes in parameters, branching ratios, and photodestruction rates.

REFERENCES

Adamczyk, B., Boerboom, A. J. H., Schram, B. L., and Kistemaker, J. 1966, *J. Chem. Phys.*, **44**, 4640.
Black, J. H., and Dalgarno, A. 1973*a*, *Ap. J.* (*Letters*), **184**, L101.
———. 1973*b*, *Ap. Letters*, **15**, 79.
Bless, R. C., and Savage, B. D. 1972, *Ap. J.*, **171**, 293.
Bolden, R. C., and Twiddy, W. D. 1972, *Faraday Disc.*, **53**, 192.
Brown, R. L., and Gómez-González, J. 1974, *Ap. J.*, **188**, 475.
Burt, J. A., Dunn, J. L., McEwan, M. J., Sutton, M. M., Roche, A. E., and Schiff, H. I. 1970, *J. Chem. Phys.*, **52**, 6062.
Crutcher, R. M., and Watson, W. D. 1976, *Ap. J.* (*Letters*), in press.
Dalgarno, A., Oppenheimer, M., and Berry, R. S. 1973, *Ap. J.* (*Letters*), **183**, L21.
Davies, R. D., and Mathews, H. E. 1972, *M.N.R.A.S.*, **156**, 253.
de Jong, T. 1972, *Astr. and Ap.*, **20**, 263.
Fehsenfeld, F. C., Dunkin, D. B., Ferguson, E. E., and Albritton, D. L. 1973, *Ap. J.* (*Letters*), **183**, L25.
Fehsenfeld, F. C., and Ferguson, E. E. 1972, *J. Chem. Phys.*, **56**, 3066.
Fehsenfeld, F. C., Schmeltkopf, A. L., and Ferguson, E. E. 1967, *J. Chem. Phys.*, **46**, 2802.
Ferguson, E. E. 1973, *Atomic Data and Nuclear Data Tables*, **12**, 159.
Field, G., and Steigman, G. 1971, *Ap. J.*, **166**, 59.
Glassgold, A. E., and Langer, W. D. 1973, *Ap. J.*, **186**, 859.
———. 1974, *ibid.*, **193**, 73.
———. 1975, *ibid.*, **197**, 347.
Herbig, G. 1968, *Zs. f. Ap.*, **68**, 243.
Herbst, E., and Klemperer, W. 1973, *Ap. J.*, **185**, 505.
Hobbs, L. M. 1973, *Ap. J.*, **181**, 795.
Hollenbach, D. J., Werner, M., and Salpeter, E. E. 1971, *Ap. J.*, **163**, 165.
Hollis, J. M., Snyder, L. E., and Ulich, B. L. 1975, *Bull. AAS*, **7**, 540.

Hudson, R. D. 1971, *Rev. of Geophys. and Space Sci.*, **9**, 306.
Huntress, W. T. 1976, preprint.
Jenkins, E. B., Drake, J. F., Morton, D. C., Rogerson, J. B., Spitzer, L., and York, D. G. 1973, *Ap. J.* (*Letters*), **181**, L122.
Johnsen, R., and Biondi, M. A. 1974, *J. Chem. Phys.*, **61**, 2112.
Jura, M. 1974*a*, *Ap. J.* (*Letters*), **190**, L33.
———. 1974*b*, *Ap. J.*, **191**, 375.
Jura, M., and Dalgarno, A. 1971, *Astr. and Ap.*, **14**, 243.
Kim, J. K., Theard, L. P., and Huntress, W. T. 1975, *J. Chem. Phys.*, **62**, 45.
Langer, W. D. 1976*a*, *Ap. J.*, in press.
———. 1976*b*, in preparation.
Laudenslager, J. B., Huntress, W. T., and Bowers, M. T. 1974, *J. Chem. Phys.*, **61**, 4600.
Leu, M. T., Biondi, M. A., and Johnsen, R. A. 1973*a*, *Phys. Rev.*, **7A**, 292.
———. 1973*b*, *ibid.*, **8A**, 420.
Morton, D. C. 1975, *Ap. J.*, **197**, 85.
Morton, D. C., Drake, J. F., Jenkins, E. B., Rogerson, J. B., Spitzer, L., and York, D. G. 1973, *Ap. J.* (*Letters*), **181**, L103.
Neynaber, R. H., and Trujillo, S. M. 1968, *Phys. Rev.*, **167**, 63.
O'Donnell, E. J., and Watson, W. D. 1974, *Ap. J.*, **191**, 89.
Rogerson, J. B., and York, D. G. 1973, *Ap. J.* (*Letters*), **186**, L95.
Sancisi, R., Goss, W. M., Anderson, C., Johansson, L. E. B., and Winnberg, A. 1974, *Astr. and Ap.*, **35**, 445.
Smith, A. M., and Stecher, T. P. 1971, *Ap. J.* (*Letters*), **164**, L64.
Smith, F. J. 1966, *Planet. and Sp. Sci.*, **14**, 929.
Smith, W. H., and Stella, G. 1975, preprint, Princeton University Observatory.
Snow, T. P. 1975, *Ap. J.* (*Letters*), **201**, L21.
Snyder, L. 1975, private communication.
Solomon, P. 1974, private communication.
Solomon, P., and Klemperer, W. 1972, *Ap. J.*, **178**, 389.
Solomon, P., and Werner, M. 1971, *Ap. J.*, **165**, 41.
Spitzer, L. 1968, *Diffuse Matter in Space* (New York: Interscience).
Spitzer, L., and Cochran, W. D. 1973, *Ap. J.* (*Letters*), **186**, L23.
Spitzer, L., Cochran, W. D., and Hirshfeld, A. 1974, *Ap. J. Suppl.*, **266**, 759.
Spitzer, L., Drake, J. F., Jenkins, E. B., Morton, D. C., Rogerson, J. B., and York, D. G. 1973, *Ap. J.* (*Letters*), **181**, L116.
Stephens, T. L., and Dalgarno, A. 1972, *J. Quant. Spectrosc. and Rad. Transf.*, **12**, 569.
Stief, L. J., Donn, B., Glicker, S., Gentieu, E. P., and Mentall, J. E. 1972, *Ap. J.*, **171**, 21.
Turner, B. 1974, private communication.
Watson, W. D. 1973*a*, *Ap. J.* (*Letters*), **182**, L73.
———. 1973*b*, *ibid.*, **183**, L17.
———. 1974, *Ap. J.*, **188**, 35.
Watson, W. D., and Salpeter, E. E. 1972*a*, *Ap. J.*, **174**, 321.
———. 1972*b*, *ibid.*, **175**, 659.
Weisheit, J. C. 1973, *Ap. J.*, **185**, 877.
York, D. G., Drake, J. F., Jenkins, E. B., Morton, D. C., Rogerson, J. B., and Spitzer, L. 1973, *Ap. J.* (*Letters*), **182**, L1.

A. E. GLASSGOLD: Physics Department, New York University, 4 Washington Place, New York, NY 10003
WILLIAM LANGER: Goddard Institute for Space Studies, 2880 Broadway, New York, NY 10025